Anal. Bioanal. Electrochem., Vol. 13, No. 2, 2021, 202-213

Analytical &
Bioanalytical
Electrochemistry

2021 by CEE
www.abechem.com

Full Paper

Effect of The Free Water Content in Biodiesel On the Corrosion of Copper and AISI 1045 Steel: An Approach Using the Biodiesel/KOH-Solution Interface

Luis Díaz-Ballote,[1,*] and Juan Genesca[2]

[1]*Departamento de Fascia, Centro de Investigación y de Estudios Avanzados del Instituto Politécnico Nacional - Unidad Mérida, Mérida, Yucatán, 97310, Mérida, Yuc., México*
[2]*Polo Universitario de Tecnología Avanzada. Facultad Química. Universidad Nacional Autónoma de México, UNAM. 66629 Apodaca. Nuevo León. México*

*Corresponding Author, Tel.: +52 (999) 942 9437; Fax: +52 (999) 981 2917
E-Mail: luisdiaz@cinvestav.mx

Received: 14 January 2021 / Received in revised form: 16 September 2021 /
Accepted: 20 September 2021 / Published online: 30 September 2021

Abstract- Electrochemical measurements in low conductive media, such as biodiesel, are challenging. Here, the electrochemical corrosion process of carbon steel and copper, due to the free water content in biodiesel storage tanks, is studied. The electrochemical analysis was carried out at the interface of the biodiesel and a KOH aqueous solution under controlled experiments that replicate the free water content in biodiesel. The main contribution of this work is a movable working electrode in a typical three-electrode cell configuration for electrochemical characterization purposes. Corrosion of copper and AISI 1045 carbon steel was investigated using three standard electrochemical techniques, open circuit potential, potentiodynamic polarization, and electrochemical impedance spectroscopy. The working electrode was placed on a translation stage provided with a micrometer that allowed measurements at different points of the interface. Copper (4.0 $\mu A \cdot cm^2$) was found to be more prone to corrosion than carbon steel (0.03 $\mu A \cdot cm^2$). The results demonstrate that the novel proposed experimental setup provides a reliable option to study the corrosion of metals exposed to biodiesel.

Keywords- Electrochemical methods; Biofuels; Movable electrode; Oily film

---

1. INTRODUCTION

Biodiesel is defined as a mixture of fatty acid methyl esters (FAMEs) derived from vegetable oils or animal fats (triglycerides) [1]. Biodiesel is produced by the well-known transesterification reaction, by which the triglycerides are reacted with short-chain alcohol (methanol or ethanol) in the presence of a catalyst (KOH or NaOH) [2]. Both homogeneous and heterogeneous catalysts can be used for the transesterification reaction [3]. One of the most used homogeneous alkali catalysts is potassium hydroxide, KOH. Biodiesel has been recognized as a bio-renewable, non-toxic, and biodegradable alternative to petrodiesel [4,5]. However, biodiesel has been found more corrosive in comparison to petrodiesel [6]. The hygroscopic property of biodiesel is a serious concern [7,8]. According to Fregolente [9], biodiesel can absorb up to 6.5 times more water as compared to diesel. The presence of water in biodiesel can promote corrosion of the fuel system [10,11], affecting its effective lifetime. Although biodiesel corrosiveness is determined by the copper strip corrosion test [12], corrosion of metals in biodiesel is commonly investigated, measuring weight changes after long-term exposure [13–15]. Nevertheless, a growing alternative is the use of electrochemical methods [16–20], which have several advantages that make them attractive for biodiesel characterization; such as the relatively short time to obtain useful information on the material corrosion properties, and the simplicity and reliability of the technique. However, the high electrical resistance of biodiesel represents a serious problem to carry out electrochemical measurements. Due to this low conductivity the corrosion rate of metals immersed in biodiesel obtained by this technique can be misleading. Various experimental strategies, aiming to overcome the drawback of the low conductivity of biodiesel, have been proposed.

Corrosion of carbon steel at the biodiesel/tap or biodiesel/simulated seawater interface was successfully studied using wire beam electrode technique (WBE) by Wang et al. [21,22]. Moreover, it has been reported that the presence of contaminants in biodiesel could increase the conductivity of biodiesel allowing the electrochemical measurements [23]. In the present work, an approach to testing corrosion resistance of metals such as AISI 1045 steel and copper in contact with biodiesel, water, and potassium hydroxide (as a contaminant) is reported. Both metals were used as working electrodes to demonstrate the utility of the experimental setup proposed. The study was conducted in a layer of biodiesel over a KOH aqueous solution because the density of biodiesel, 0.86 – 0.90 g cm-3 (EN 14214:2003) is lower than water. Electrochemistry was used to obtain information from the KOH solution, as well as the KOH-solution/biodiesel interface. The experimental setup used in this work is a novel proposal for studying the corrosion of metals in contact with a biofuel and is part of the efforts to allow the use of ordinarily available techniques for this kind of measurements.

2. EXPERIMENTAL SECTION

2.1. Biodiesel Preparation

Biodiesel was prepared from commercial soybean oil by a typical alkaline transesterification process, following a procedure that has been described elsewhere [23]. Soy-based biodiesel was used in this study because its composition is considered representative of most of the biodiesels. The experiments were designed to simulate the typical conditions of biodiesel storage tanks.

2.2. Materials

Potassium hydroxide and methanol were purchased from Sigma-Aldrich. Samples of copper, Cu (99.9 %), were cut from a Cu rod with diameter of 5.0 mm; acquired from Goodfellow Materials, Ltd. Pieces of 1.0 x 1.0 cm^2 of AISI 1045 steel (0.43-0.50 wt.% C, 0.60-0.90 wt.% Mn, 0.05 wt.% (max) S, 0.04 wt.% (max) P, balance Fe) hereafter referred to as carbon steel, CS, were cut from a carbon steel sheet purchased in a local steel supplier. Samples of Cu and CS were embedded in epoxy resin to give an exposed area of 0.196 cm^2 (0.5 cm outside diameter) and 1.0 x 1.0 cm^2 , respectively. Before the electrochemical experiments, the Cu and CS samples were wet-abraded with emery paper (220, 400 and 600 grit), rinsed with distilled water, degreased with acetone, and dried with hot air.

2.3. Electrochemical Measurements

A three-electrode setup cell with two compartments was used for the electrochemical measurements (Fig. 1). The main compartment contained a 0.1 M KOH solution, the working electrode, biodiesel, and a platinum foil as an auxiliary electrode. The secondary compartment was used only for the reference electrode (saturated calomel electrode, SCE). First, the KOH solution was poured into the main compartment; afterwards, the working and platinum electrodes were immersed. On the last step, biodiesel was gently poured to form a layer over the KOH solution. The reference electrode, SCE was located on the other side of the cell. A Luggin capillary allowed the ionic conduction and reduced contamination between compartments. The working electrode was attached to a micrometer that allowed it to be moved up or down.

During the experiments, the working electrode was moved stepwise, starting in the aqueous solution and going through the interface water/biodiesel. For all the testes, the working electrode was initially placed in the KOH aqueous solution, with the purpose to start at a biodiesel-free region. Electrochemical measurements were carried out using a Gamry PCI4-300 potentiostat/galvanostat (Gamry Instruments, Inc., USA). The measures were carried out in selected points using the sequencing wizard of the Gamry framework system in the following order: open-circuit potential (OCP), electrochemical impedance spectroscopy (EIS), and potentiodynamic polarization. The OCP was recorded for 300s. EIS was performed in the frequency range from 100 kHz to 200 mHz, using a sine wave amplitude of 10 mV at the open-circuit potential. The potentiodynamic polarization was carried out from - 250 mV to 250 mV at the OCP with a scan rate of 1 $mV \cdot s^{-1}$. The electrochemical test was replicated three times using a polished sample, fresh KOH solution and neat biodiesel.

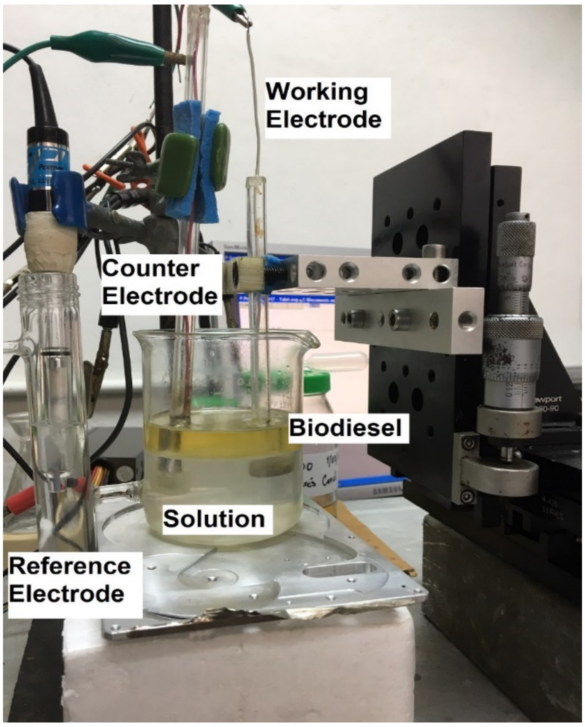

Fig. 1. Photograph of the experimental arrangement, showing the main elements.

3. RESULTS AND DISCUSSION

3.1. Open-Circuit Potential

The anodic and cathodic reaction rates determine the OCP in which both reaction rates are equal. The typical OCP behavior of Cu and CS is shown in Fig. 2. As the working electrode approaches the KOH-solution/biodiesel interface (from the pure KOH solution region) both, Cu and CS samples, display an increasing OCP towards the noble direction. A potential explanation of this behavior is the formation of a protective layer due to the alkaline solution [24,25], along with a growing oily film over the electrode as it goes closer to the KOH-solution/biodiesel interface. In addition, Fig. 2 shows that the OCP of CS is always located at more negative values as compared to that of the Cu sample. Interestingly, at the bulk of the biodiesel, the OCP of CS shifted slightly to more negative potentials and presented instability. These results suggest a different behavior of the oxide film between Cu and CS in the presence of OH^- ions, which decreases towards the KOH-solution/biodiesel interface.

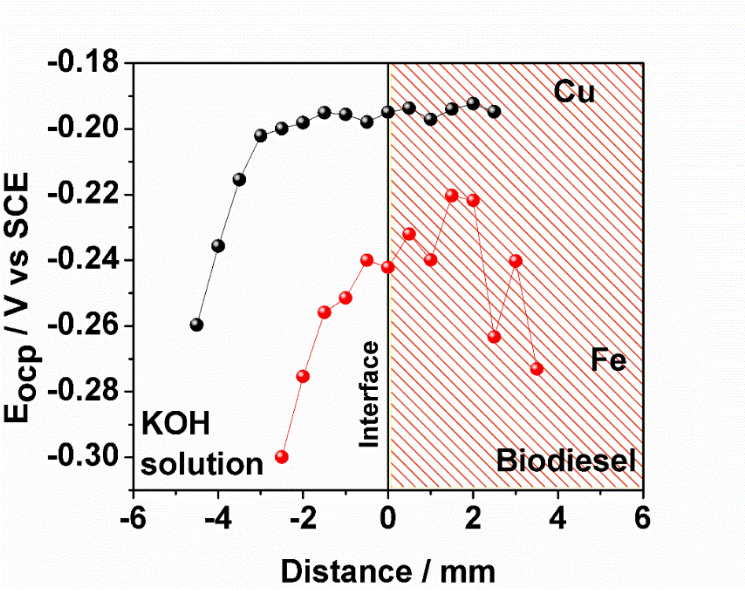

Fig. 2. Open-circuit potential of Cu and CS as a function of the distance to the KOH-solution/biodiesel interface.

3.2. Open-Circuit Potential

Typical polarization curves of CS and Cu at different distances through the KOH solution/biodiesel interface are shown in Fig. 3. The test starts with the working electrode (WE) immersed in the KOH solution; following, the working electrode is moved up in steps of 0.5 mm, towards the biodiesel bulk. The working electrode is allowed to remain for 60 s in each point before the measurement. The experimental setup allows the investigation of the gradual effect of biodiesel on the corrosion behavior of CS and Cu. The anodic branch of the polarization curves of both, CS and Cu, electrodes exhibit an active-passive region that is the typical shape of a working electrode forming a protective layer in KOH solutions [25,26]. It is also observed from Fig. 3 that the corrosion rate of Cu is faster than that of CS. The high corrosion rate of Cu suggests that formation of soluble species of Cu [27,28] are faster than soluble species from the CS. A widely observed reason for the Cu poor protective film, in alkaline solutions, is the presence of porous, which allow Cu^{2+} dissolution [29,30]. On the other hand, a thin and highly protective film is formed on CS while in contact with an alkaline solution [31]. In fact, the properties of the passive film are the key factors for application of CS as reinforcement steel in concrete [32,33]. Moreover, when the electrode is placed closer to the biodiesel bulk, the active region disappears, while the anodic current keeps decreasing. This behavior is attributed to a decrease of the OH^- ions [25], needed for the film formation; as well as surface adsorption of biodiesel into the metal surface, which supports the low passive current (i_{pc}).

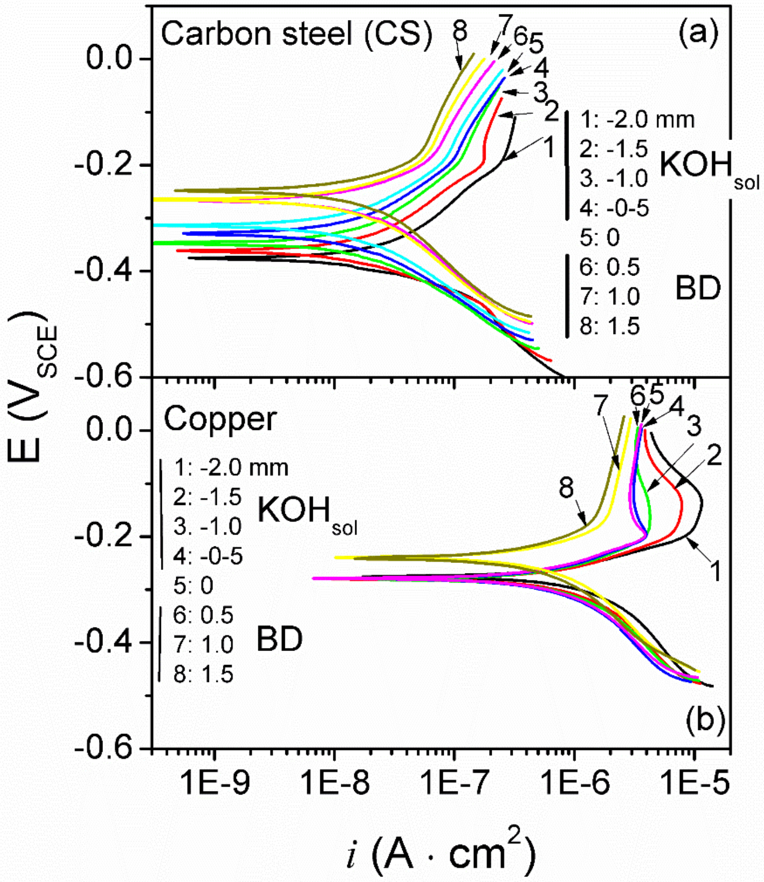

Fig. 3. Tafel plots of a) carbon steel and b) Copper, at different locations through the KOH-solution/biodiesel interface (negative distances indicate that the electrode is immersed in the KOH solution).

Fig. 4 shows the behavior of the corrosion potential (E_{corr}) and corrosion current density (i_{corr}) for CS and Cu as a function of the position, below and above, from the KOH-solution/interface. These parameters were calculated assuming kinetic control and fitting the Bultler-Volmer equation to the experimental data. The E_{corr} of CS and Cu moves toward noble potentials, as the working electrode goes toward the biodiesel bulk. This is likely due to a reduction of the reaction area because of the growing oily film. The i_{corr} decreases slightly for both metals as the working electrode moves toward the biodiesel, in agreement with the polarization measurements showed in Fig. 3. Comparison of the current density, for CS (0.03 $\mu A\cdot cm^2$) and Cu (4.0 $\mu A\cdot cm^2$), show that Cu is more prone to corrosion than CS in this media. These results agree well with various studies on metal corrosion in biodiesel, based on weight loss of coupons exposed to long-term storage, which indicate that Cu is more susceptible to corrosion than low CS [10,34–36].

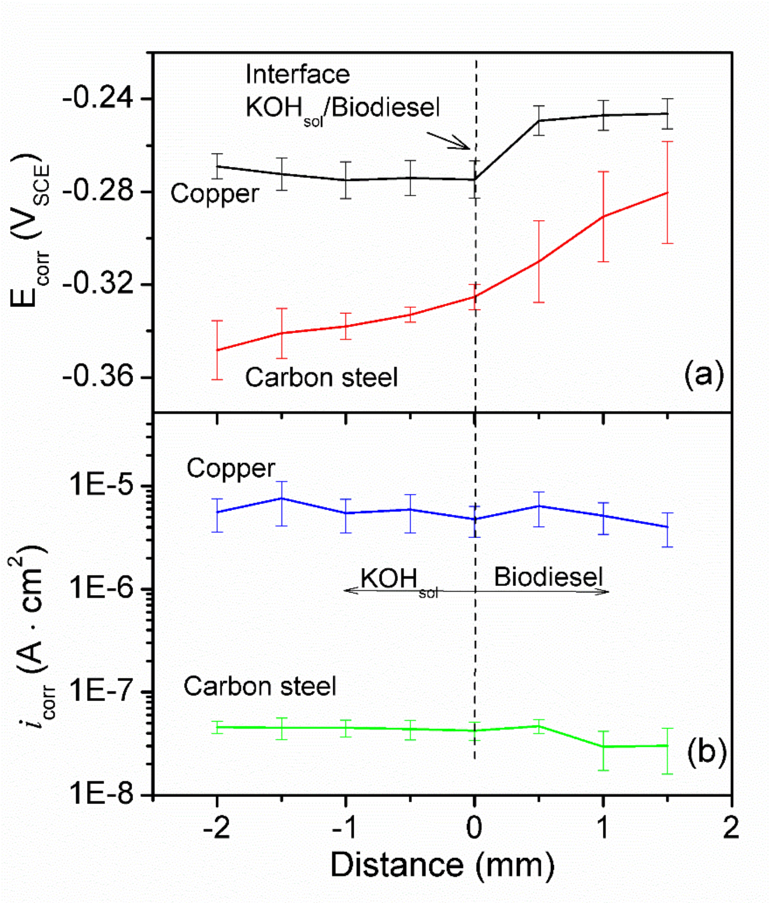

Fig. 4. Average values of a) the corrosion potential, E_{corr}; and b) the corrosion current density, i_{corr}, of Cu and CS with the distance to the KOH-solution/biodiesel interface (negative distances indicate that the electrode is in the KOH solution).

3.3. Electrochemical Impedance Spectroscopy

Typical Bode plots of Cu and CS acquired at different positions with respect to the KOH-solution/biodiesel interface are shown in Fig. 5. The impedance spectra 1, 2, 3, 4, and 5, correspond to cases where the working electrode was immersed in the KOH solution, while impedance spectra 6, 7, and 8 belong to those where the electrode is immersed in biodiesel. The scale of the Bode plot of CS is about 10 times larger than that of Cu. It can also be noted that, as the electrode approaches the biodiesel bulk, the impedance increases, which evidences an increment in the film resistance (R_f) and the charge transfer resistance (R_{ct}). This result is in agreement with the low conductivity of the biodiesel, which becomes the major component in the mixture.

The presence of a protective layer observed in the polarization measurements, and the electrochemical impedance data were the criteria to choose the equivalent circuit used in this study (Fig. 6). Furthermore, similar impedance data have been modelled in the literature with the equivalent circuit proposed [37–40].

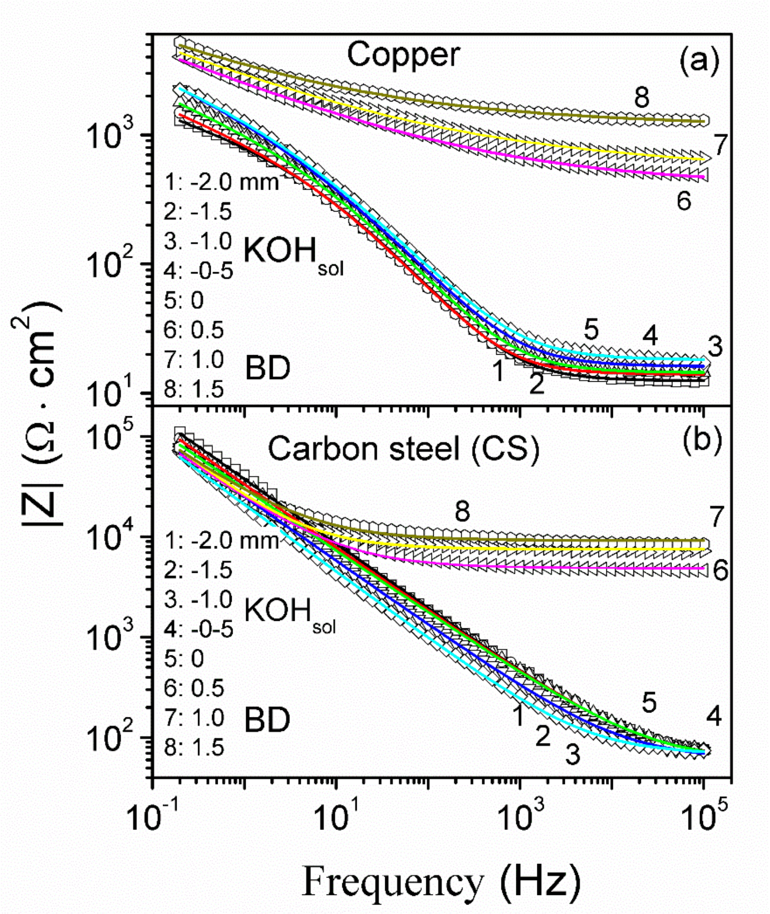

Fig. 5. Bode plots of a) Copper and b) carbon steel immersed in biodiesel as a function of the distance to the KOH-solution/biodiesel interface. Symbols and solid lines represent the experimental data and fits, respectively.

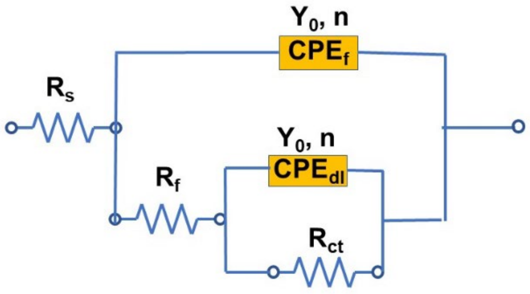

Fig. 6. Electrical equivalent circuit used to fit the obtained impedance spectra of Cu and CS.

The equivalent circuit includes two constant phase elements (CPE), one for the film (CPE$_f$), and another one associated to the double layer (CPE$_{dl}$). The CPEs are characterized by Y_0 with units of mS·cm^{-2}·s^n; the n value accounts for surface inhomogeneities. The resistive element (R$_s$) represents the solution resistance, (R$_f$) the film resistance, and (R$_{ct}$) the charge-transfer resistance. The fitting parameters of Cu and CS obtained from the EIS spectra are presented in Tables 1 and 2, respectively. Importantly, the goodness-of-fit values obtained are in the order of 10^{-3} for both Cu and CS. In addition, to demonstrate that the system fulfilled the required conditions (linearity, stability, and causality) in the impedance measurements, the results gathered were validated through the use of a Kramers–Kronig analysis program. In Tables 1 and 2, one can observe the influence of the biodiesel concentration on the solution resistance (R_s) and the charge transfer resistance (R_{ct}); for both, Cu and CS. The R_s increases in both cases, as expected, when the solution is rich in biodiesel. The R_{ct} increases with the biodiesel content up to 671 MΩ cm^2 (distance to the interface: 1.5 mm) for Cu, Table 1. On the other hand, for CS (Table 2), the addition of biodiesel results in an approximately constant value in the order of $20 \cdot 10^3$ MΩ cm^2, as the electrode is immersed in biodiesel.

Table 1. Fitting parameters obtained from the impedance spectra of the Copper electrode around the KOH- solution/biodiesel interface.

Distance (mm)	R_s (Ω cm^2)	R_f (Ω cm^2)	CPE$_f$		R_{ct} (MΩ cm^2)	CPE$_{dl}$	
			Yo (μS s^n cm^{-2})	n		Yo (μS s^n cm^{-2})	n
1.5	1531 (± 376.2)	2.0 (± 1.5)	178.3 (± 117.5)	0.44	671.1 (± 177.0)	285.3 (± 166.5)	0.75
1	1163 (± 353.8)	0.7 (± 0.56)	167.7 (± 112.9)	0.49	178 (± 48.0)	246.6 (± 149.9)	0.59
0.5	772 (± 157.6)	0.4 (± 0.25)	134.4 (± 86.2)	0.54	299 (± 141)	206.3 (± 118.3)	0.47
0	9.7 (± 3.4)	2.0 (± 1.8)	109.9 (± 65.7)	0.70	9 (± 5.0)	167.7 (± 78.9)	0.60
-0.5	11.3 (± 2.5)	0.1 (± 0.08)	81.7 (± 42.7)	0.72	5 (± 2.7)	181.4 (± 72.2)	0.55
-1	10.7 (± 2.2)	0.06 (± 0-05)	71.0 (± 57.9)	0.75	1 (± 0.6)	131.1 (± 63.8)	0.52
-1.5	10.4 (± 2.0)	0.04 (± 0-03)	61.4 (± 50.1)	0.77	0.2 (± 0.1)	120.7 (± 58.7)	0.51
-2	9.3 (± 1.8)	0.05 (± 0.04)	55.9 (± 45.69)	0.77	0.2 (± 0.1)	118.5 (± 58.0)	0.49

In general, the polarization resistance, $R_p = R_f + R_{ct}$ [37], increases as the electrode is moved towards the biofuel phase. As observed, far away from the boundaries of the KOH-solution/biodiesel interface, increasing the amount of biodiesel increases the charge transfer resistance (R_{ct}), mainly in CS. Seemingly, a critical factor that may be contributing to the decrease in the conductivity of the medium, when the biodiesel phase is predominant, could be the formation of an insulating film on the surfaces of the Cu and CS electrodes. Therefore, the increasing R_{ct} values have been related to the increasing amount of the biodiesel plus a decrease of water drops mobility in the KOH solution, hampering the charge transport [19,41]. The dependence of the R_s values with the distance exhibit similar behavior to R_f and R_{ct}. This is in well with an increased biodiesel concentration hampering the charge transfer at the metal surface. Interestingly, the latter can justify the second capacitive arc that appears in the low-frequency range, which is characteristic of the species adsorbed on the metal surface that form an insulating layer [42].

Table 2. Fitting parameters obtained from the impedance spectra of the carbon steel electrode around the KOH- solution/biodiesel interface.

Distance (mm)	R_s (Ω cm^2)	R_f (kΩ cm^2)	CPE_f		R_{ct} (MΩ cm^2)	CPE_{dl}	
			Yo (μS s^n cm^{-2})	n		Yo (μS s^n cm^{-2})	n
1.5	2826 (± 2304)	140.9 (± 97)	1.1 (± 1.0)	0.78	23863 (± 9426)	7.5 (± 2.2)	0.50
1	2404 (± 1935)	14.8 (± 5)	1.4 (± 1.1)	0.57	24350 (± 13480)	9.4 (± 0.5)	0.69
0.5	1620 (± 1262)	11.1 (± 2)	5.6 (± 2.7)	0.58	27086 (± 21303)	5.5 (± 2.3)	0.81
0	42 (± 12)	25.2 (± 18)	6.2 (± 2.2)	0.70	9312 (± 7506)	4.3 (± 1.8)	0.71
-0.5	51 (± 4)	52.4 (± 19)	7.8 (± 0.6)	0.71	87 (± 70)	1.9 (± 0.9)	0.68
-1	50 (± 3)	51.0 (± 10)	7.2 (± 1.7)	0.72	11 (± 8.4)	4.4 (± 1.2)	0.78
-1.5	50 (± 3)	50.0 (± 17)	6.8 (± 0.8)	0.72	5 (± 3.2)	2.1 (± 0.7)	0.72
-2	51 (± 3)	43.2 (± 18)	4.1 (± 2.0)	0.82	42 (± 33.1)	4.7 (± 1.7)	0.64

4. CONCLUSION

The use of a movable working electrode allowed the observation of substantial differences in the corrosion process of Cu and CS immersed in biodiesel. The corrosion rate of Cu in biodiesel was observed to be at least one order of magnitude larger than that of CS, in the same conditions. As compared to CS, Cu was found more susceptible to corrosion in the KOH-solution/biodiesel interface, in well agreement with previous reports. These results demonstrate that the experimental setup proposed in the present study is a reliable alternative to investigate the corrosion of metals exposed to biodiesel contaminated with water. Moreover, it was shown that the use of a movable working electrode allows the application of various electrochemical methods to investigate the corrosion of metals immersed in biodiesel.

Acknowledgements

The measurements were performed on the electrochemical systems acquired through CONACYT grant 205050/2013.

Declarations of Interest

The authors declare no conflict of interest in this reported work.

REFERENCES

[1] S. K. Hoekman, A. Broch, C. Robbins, E. Ceniceros, and M. Natarajan, Renew. Sustain. Energy Rev. 16 (2012) 143.

[2] G. Vicente, and M. Martínez, J. Aracil, Bioresour. Technol. 92 (2004) 297.

[3] M. K. Lam, K. T. Lee, and A.R. Mohamed, Biotechnol. Adv. 28 (2010) 500.

[4] A. Demirbas, Prog. Energy Combust. Sci. 31 (2005) 466.

[5] J. Janaun, and N. Ellis, Renew. Sustain. Energy Rev. 14 (2010) 1312.

[6] M. A. Fazal, A. S. M. A. Haseeb, and H. H. Masjuki, Fuel Process. Technol. 91 (2010) 1308.

[7] M. A. Fazal, A. S. M. A. Haseeb, and H. H. Masjuki, Renew. Sustain. Energy Rev. 15 (2011) 1314.

[8] F. Sundus, M. A. Fazal, and H. H. Masjuki, Renew. Sustain. Energy Rev. 70 (2017) 399.

[9] P. B. L. Fregolente, L. V. Fregolente, and M. R. Wolf Maciel, J. Chem. Eng. Data. 57 (2012) 1817.

[10] A. S. M. A. Haseeb, H. H. Masjuki, L. J. Ann, and M. A. Fazal, Fuel Process. Technol. 91 (2010) 329.

[11] A. S. M. A. Haseeb, M. A. Fazal, M.I. Jahirul, and H. H. Masjuki, Fuel 90 (2011) 922–931.

[12] G. Knothe, JAOCS, J. Am. Oil Chem. Soc. 83 (2006) 823.

[13] E. S. Almeida, F. M. Portela, R. M. F. Sousa, D. Daniel, M. G. H. Terrones, E. M. Richter, and R. A. A. Muñoz, Fuel 90 (2011) 3480.

[14] D. Jin, X. Zhou, P. Wu, L. Jiang, and H. Ge, Renew. Energy. 81 (2015) 457.

[15] S. Deshpande, A. Joshi, S. Vagge, and N. Anekar, Eng. Fail. Anal. 105 (2019) 1319.

[16] A. H. Akita, C. S. Fugivara, I. V. Aoki, and A. V. Benedetti, Using the Electrochemical Impedance Spectroscopy to Characterize Carbon Steel in Biodiesel Medium, in: ECS Trans. (2012) bll 71.

[17] M. A. Deyab, J. Taiwan Inst. Chem. Eng. 58 (2016) 536.

[18] M. A. Deyab, and S. T. Keera, J. Taiwan Inst. Chem. Eng. 68 (2016) 187.

[19] T. C. Pereira, J. R. Delfino, A. A. P. Ferreira, F. J. S. Barros, E.P. Marques, J. Zhang, and A. L. B. Marques, Electroanalysis 29 (2017) 814.

[20] S. Deshpande, A. Joshi, S. Vagge, and N. Anekar, Mater. Today Proc. (2020).

[21] W. Wang, X. Zhang, and J. Wang, Mater. Corros. 60 (2009) 957.

[22] W. Wang, P.E. Jenkins, and Z. Ren, Corros. Sci. 57 (2012) 215.

[23] L. Díaz-Ballote, J. F. López-Sansores, L. Maldonado-López, and L. F. Garfias-Mesias, Electrochem. Commun. 11 (2009) 41.

[24] W.A. Badawy, Corrosion 55 (1999) 268.

[25] A. Fattah-alhosseini, A. Jalali, and S. Felegari, Arab. J. Sci. Eng. 40 (2015) 2985.

[26] A. Fattah-alhosseini, and O. Imantalab, Metall. Mater. Trans. A Phys. Metall. Mater. Sci. 47 (2016) 572.

[27] J. Ambrose, R.G. Barradas, and D.W. Shoesmith, J. Electroanal. Chem. 47 (1973) 47.

[28] M. Shirkhanzadeh, G. E. Thompson, and V. Ashworth, Corros. Sci. 31 (1990) 293.

[29] M. Biton, G. Salitra, D. Aurbach, P. Mishkov, and D. Ilzycer, J. Electrochem. Soc. 153 (2006) B555.

[30] D. W. Shoesmith, S. Sunder, M. G. Bailey, G. J. Wallace, and F. W. Stanchell, J. Electroanal. Chem. 143 (1983) 153.

[31] L. Freire, X. R. Nóvoa, M. F. Montemor, and M. J. Carmezim, Mater. Chem. Phys. 114 (2009) 962.

[32] S. Chakri, I. Frateur, M. E. Orazem, E. M. M. Sutter, T. T. M. Tran, B. Tribollet, and V. Vivier, Electrochim. Acta 246 (2017) 924.

[33] M. Liu, X. Cheng, G. Zhao, X. Li, and Y. Pan, Surf. Interface Anal. 48 (2016) 981.

[34] D. P. Geller, T. T. Adams, and J. W. Goodrum, J. Pendergrass, Fuel 87 (2008) 92.

[35] D. M. Fernandes, R. H. O. Montes, E. S. Almeida, A. N. Nascimento, P. V. Oliveira, E. M. Richter, and R. A. A. Muñoz, Fuel 107 (2013) 609.

[36] D. L. Cursaru, G. Brănoiu, I. Ramadan, and F. Miculescu, Ind. Crops Prod. 54 (2014) 149.

[37] A. Fattah-Alhosseini, and S. Alizad, Anal. Bioanal. Electrochem. 7 (2015) 415.

[38] F. Rosalbino, R. Carlini, F. Soggia, G. Zanicchi, and G. Scavino, Corros. Sci. 58 (2012) 139.

[39] M. Sánchez, J. Gregori, M.C. Alonso, J. J. García-Jareño, and F. Vicente, Electrochim. Acta 52 (2006) 47.

[40] Q. Zeng, J. Sun, W. Emori, and S. L. Jiang, J. Mater. Eng. Perform. 25 (2016) 1773.

[41] T. C. Pereira, C. A. F. Conceição, A. Khan, R. M. T. Fernandes, M. S. Ferreira, E. P. Marques, and A. L. B. Marques, Spectrochim. Acta - Part A Mol. Biomol. Spectrosc. 168 (2016) 60.

[42] J. R. Delfino, T. C. Pereira, H. D. Costa Viegas, E. P. Marques, A. A. Pupim Ferreira, L. Zhang, J. Zhang, and A. L. Brandes Marques, Talanta. 179 (2018) 753.